HHS Public Access

Author manuscript

Brain Stimul. Author manuscript; available in PMC 2021 September 01.

Published in final edited form as:

Brain Stimul. 2020 ; 13(5): 1232–1244. doi:10.1016/j.brs.2020.06.002.

A systematic exploration of parameters affecting evoked intracranial potentials in patients with epilepsy

Bornali Kundu, MD, PhD[*,1], **Tyler S. Davis, MD, PhD**[*,1], **Brian Philip**[2], **Elliot H. Smith, PhD**[1], **Amir Arain, MD**[3], **Angela Peters, MD**[3], **Blake Newman, MD**[3], **Christopher R. Butson, PhD**[1,2,4], **John D. Rolston, MD, PhD**[1,2,4]

[1]Department of Neurosurgery, Clinical Neurosciences Center, University of Utah, Salt Lake City, Utah, USA

[2]Department of Biomedical Engineering, University of Utah, Salt Lake City, Utah, USA

[3]Department of Neurology, Clinical Neurosciences Center, University of Utah, Salt Lake City, Utah, USA

[4]Scientific Computing and Imaging Institute, University of Utah, Salt Lake City, Utah, USA

Abstract

Background: Brain activity is constrained by and evolves over a network of structural and functional connections. Corticocortical evoked potentials (CCEPs) have been used to measure this connectivity and to discern brain areas involved in both brain function and disease.

However, how varying stimulation parameters influences the measured CCEP across brain areas has not been well characterized.

Objective: To better understand the factors that influence the amplitude of the CCEPs as well as evoked gamma-band power (70–150 Hz) resulting from single-pulse stimulation via cortical surface and depth electrodes.

Methods: CCEPs from 4370 stimulation-response channel pairs were recorded across a range of stimulation parameters and brain regions in 11 patients undergoing long-term monitoring for

Corresponding author: Dr. John D. Rolston, Department of Neurosurgery, Clinical Neurosciences Center, University of Utah, 175 N. Medical Drive East, Salt Lake City, UT 84132, Phone: 801-581-6908, Fax: 801-581-4385, neuropub@hsc.utah.edu.

Author contributions: Bornali Kundu: Conceptualization, Methodology, Software, Validation, Formal analysis, Investigation, Writing – Original Draft, Writing – Review and Editing, Visualization, **Tyler S. Davis:** Conceptualization, Methodology, Software, Validation, Formal analysis, Investigation, Writing – Original Draft, Writing – Review and Editing, Visualization, Data Curation, **Brian Philip:** Investigation, **Elliot H. Smith:** Methodology, Software, Formal Analysis, Writing – Original Draft, **Amir Arain:** Investigation, Writing – Original Draft, **Angela Peters:** Investigation, Writing – Original Draft, **Blake Newman:** Investigation, Writing – Original Draft, **Christopher R. Butson:** Formal analysis, Writing – Original Draft, and **John D. Rolston:** Conceptualization, Methodology, Investigation, Resources, Writing – Original Draft, Writing – Review and Editing, Supervision, Project administration, Funding acquisition

*Drs. Kundu and Davis contributed equally to this work.

Conflicts of Interest

The authors confirm there are no known conflicts of interest associated with this publication and there has been no significant financial support for this work that influenced its outcome.

epilepsy. A generalized mixed-effects model was used to model cortical response amplitudes from 5 to 100 ms post-stimulation.

Results: Stimulation levels <5.5 mA generated variable CCEPs with low amplitude and reduced spatial spread. Stimulation at ≥5.5 mA yielded a reliable and maximal CCEP across stimulation-response pairs over all regions. These findings were similar when examining the evoked gamma-band power. The amplitude of both measures was inversely correlated with distance. CCEPs and evoked gamma power were largest when measured in the hippocampus compared with other areas. Larger CCEP size and evoked gamma power were measured within the seizure onset zone compared with outside this zone.

Conclusion: These results will help guide future stimulation protocols directed at quantifying network connectivity across cognitive and disease states.

Keywords

Corticocortical evoked potential (CCEP); stereoelectroencephalography (SEEG); gamma; power; single-pulse electrical stimulation (SPES)

Introduction

Dynamic network structure has supplanted modular models of localized cortical function [1]. In disease states, aberrant network activity from focally damaged tissue can influence a broad network, as is the case with focal epilepsy [2,3]. One method to quantify brain connectivity is with corticocortical evoked potentials (CCEPs) [4–6], a measure of the network's effective connectivity [7] derived by directly stimulating a cortical area and measuring responses in other brain areas. This method of single-pulse electrical stimulation (SPES) provides a reproducible measure of network strength via the features of the evoked response, which occurs in select recording points (i.e., network nodes). CCEPs have been used for language and motor mapping [8,9], defining the seizure onset zone (SOZ) [6,10], differentiating brain states [11], and inferring the degree of connectivity between brain areas [4,8,9,12]. However, we lack information regarding how changing stimulation parameters affects CCEP amplitude, shape, and propagation.

The lack of standardized stimulation parameters limits interpretation of the data, reducing its clinical utility [5,13,14]. The amplitude of stimulation may be 0.5 mA to >10 mA [6,9], which changes the charge density per phase that the tissue experiences [15]. Furthermore, the clinical use of stereotactic electroencephalography (SEEG) has increased [16], but fewer studies describe the effects of stimulation with depth or SEEG electrodes [17] than with cortical surface grids. Depth electrodes generally have a larger charge density, because of their smaller surface area [4]. Additionally, intraparenchymal depth electrodes may be positioned to stimulate either white or gray matter, and the differences between recorded responses in the two tissues types have not been addressed in humans.

To better understand the dose-response relationship between stimulation of SEEG and surface electrocorticography electrodes and the resulting CCEPs, we systematically applied SPES to intracranial electrodes in patients undergoing long-term epilepsy monitoring. We measured variations in the CCEP amplitude and waveform shape at different stimulation

amplitudes, across stimulation-response channel pairs, and across various locations in the brain. We also addressed whether the broadband, high-frequency local field potential gamma power (70-150 Hz) (also known as “high gamma-band” [18,19] or “broadband gamma” power [14]) evoked by stimulation is similarly influenced by these parameters. Evoked gamma-band power from stimulation has been explored as a measure of the evoked response [14] and as a marker of the SOZ [20], but the CCEP amplitude and gamma-band power measures have not been compared in the same dataset across brain regions.

Methods

Patients

This study was approved by the Institutional Review Board, and all patients provided informed consent (IRB procotol 00069440). Data were collected in 2018-2019 from adult patients who underwent intracranial monitoring for medically refractory epilepsy. SEEG electrodes were implanted for routine medical management. One patient also had a grid of 64 electrocorticography electrodes implanted. Data were collected at the completion of the clinical monitoring period after antiepileptic medications had been resumed and while patients were awake but resting in bed. The SOZ was determined by the treating epileptologist. Within the long-term monitoring data interpretation, if the epileptologist named particular electrodes to be within the SOZ, those contacts were then labeled as such for the experimental dataset. Thus, patients for whom the seizure onset zone could not be identified or those with regional or multifocal areas of seizure generation have no contacts labeled as within the SOZ in the experimental dataset.

Electrodes

SEEG electrodes consisted of 4-10 platinum contacts (Ad-Tech Corp., Racine, WI) arranged in a linear array. The grid consisted of 64 platinum discs (1-cm spacing, 8×8-grid) and a 4.2-mm^2 exposed recording surface area embedded in a polyurethane substrate (Ad-Tech Corp.). To identify the electrode location, each patient’s structural T1 spoiled gradient recalled or magnetization-prepared rapid acquisition gradient-echo MRI was coregistered with postoperative high-resolution CT (slice thickness <1 mm) by using MATLAB (Mathworks, Natick, MA) and the Statistical Parametric Mapping toolbox (SPM12;https://www.fil.ion.ucl.ac.uk/spm/software/). MRI volumes were registered to the Montreal Neurological Institute ECBM152 template atlas using SPM12. Electrode locations were determined using labeled data from Neuromorphometrics, Inc.(http://Neuromorphometrics.com). Electrode locations relative to gray versus white matter were determined using the coregistered tissue probability maps in SPM12. Anatomical region was categorized into white matter, neocortex, hippocampus, and amygdala for each channel.

Recording

Neurophysiological data were recorded using a 128-channel data acquisition system (NeuroPort, Blackrock Microsystems, Salt Lake City, UT), and stimulation was delivered using a 96-channel stimulation system (Cerestim, Blackrock Microsystems). Recorded data were bandpass filtered at 0.3-250 Hz and sampled at 1 kHz.

For each patient, a single intracranial depth electrode contact was chosen to be the reference channel. We chose intracranial electrodes for reference because the signal was considerably cleaner than that derived from a scalp or skin electrode. The reference electrode was always located deep in white matter and without artifact or epileptiform activity.

Stimulation

Monopolar stimulation was applied to 404 contacts across all patients as a single cathodic-first biphasic pulse (0.5 ms/phase) with a randomized interpulse interval (2.5-3.5 sec) using custom software written in Labview (National Instruments, Austin, TX). The majority of electrodes had a surface area of 7.35 mm^2 (range 4.15 – 10.45 mm^2). The charge per phase from stimulation over a range of 2.5 – 10 mA was 1.25 to 5 μC and the charge density per phase was from 30 – 120 $\mu C/cm^2$/phase. This is comparable to that reported in the literature [5]. Monopolar stimulation was chosen because the stimulation location can be known with certainty, whereas with bipolar stimulation, stimulation occurs somewhere between the electrodes of the bipolar pair [5,18]. Modeling data suggests bipolar stimulation results in larger charge densities locally [15] compared to monopolar and may favor activation of particular fiber orientations [21].

The return (or “ground”) electrodes were selected to minimize noise and stimulation artifact. Twenty intracranial depth electrode contacts were tied together to form a very-low-impedance ground. This stimulation ground was also used as the ground for recording. Apart from the ground and reference, all other electrodes received stimulation according to the stimulation protocol. Occasionally, stimulation of an electrode that was near the dura or within the anchor bolt was noticeable to the patient or uncomfortable to the patient. Those electrodes were then removed from the stimulation protocol of that patient and not further stimulated.

“Standard” mapping used stimulation levels of 2.5-10 mA in four 2.5-mA steps across implanted electrodes. The term “level” will be used to refer to the current amplitude used for stimulation. “High-resolution” mapping used stimulation levels of 0.5-10 mA in twenty 0.5-mA steps across a subset of 2-6 electrodes. If patients received both protocols, the “standard” protocol was delivered first. For both protocols, each electrode was stimulated ≥10 times at each level, with electrode and level randomized across trials. For the “standard” protocol, stimulation location was randomized and separated from the previous 5 by ≥2 cm to avoid excessively stimulating one cortical region.

Preprocessing and data analysis

Data were divided into epochs spanning −1000 to −5 ms prestimulation and 5 to 1000 ms poststimulation, with stimulation onset at time zero. Epochs with 60-Hz noise >100 μV^2/Hz, transients >300 μV/ms, variance <1 μV^2, and voltages equal to the amplifier saturation voltage (±6553 μV) were identified as artifact and removed on a trial-by-trial basis. Channels with >50% of the epochs containing artifact were removed. Channels were also visually inspected for artifact after this automated analysis.

CCEP detection

CCEPs may have long-lasting responses [22]; we studied the early response period (<100 ms poststimulation), which has been related to structural features of network connectivity [23] and may discern the SOZ location. To detect CCEPs, each epoch was zero-phase high-pass filtered using a fourth-order, 10-Hz Butterworth filter (Supplementary Figure 1) and digitally rereferenced to the common median across all electrodes [24]. Epochs were squared, smoothed with a second-order, 10-Hz low-pass Butterworth filter, and converted back to microvolts by taking the square root, similar to [25]. A response was considered a CCEP if the trial-median of the poststimulation epochs (5-100 ms) contained at least 15 ms of uninterrupted values >3× the median (across trials and time (−100 to −5 ms)) of the prestimulation epochs, and the median (across trials and time (5-100 ms)) of the poststimulation epochs was >30 μV (Supplementary Figure 1). All stimulation-response electrode pairs that recorded a CCEP at 10 mA were kept for analysis even if a CCEP was not detected at lower levels. Pairs that did not record a CCEP at 10 mA were discarded. CCEPs on the stimulated electrodes were discarded because of artifact.

We defined several features of CCEPs. CCEP amplitude was measured as the mean absolute value 5-100 ms poststimulation using the trial-averaged waveform. Spatial spread was measured using the Euclidean distance from stimulation to any detected CCEP as calculated from the image-based channel localization. Analysis of waveform shape may provide a way of discerning the neural components that are activated with stimulation. Although CCEPs generated from epicortical grid data show N1 and N2 peaks, those components are not as prominent with SEEG electrodes so we characterized the waveform shape as a whole [14]. Pearson's correlation coefficient was used to calculate variability in the CCEP waveform shape across stimulation levels. Trial-average waveforms were derived for each channel-response pair at each level, and the correlation coefficient over time between waveforms at different levels was calculated.

Gamma-band power was calculated by bandpass filtering the poststimulation data from 70-150 Hz using a zero-phase fourth-order Butterworth filter. Epochs were rereferenced to the common median, and the Hilbert transform was applied. Average gamma-band power was obtained by multiplying the transformed data with the complex conjugate and averaging over trials and time from 5 to 100 ms poststimulation.

Statistical analysis

A generalized linear mixed-effects model was generated using data from all patients and used to analyze how stimulation parameters related to CCEP amplitude (dependent variable), while controlling for random variance across patients. Fixed effects included stimulation level, distance between stimulation and response electrodes, stimulation and response tissue types (hippocampus, amygdala, white matter, and neocortex), and whether the contacts were part of the SOZ. Patient identity was a random effect. CCEP amplitude was negatively skewed (Lilliefors test, kstat=0.1952, $p<0.001$, critical value=0.0023) and was log-transformed before applying the fit [26]. The distribution's normality was confirmed visually, but statistically, it remained significantly non-normal (Lilliefors test, kstat=0.028, $p<0.001$, critical value=0.0023), likely because of the large sample size. The model was

expressed with the following Wilkinson notation: F~1+A+B+C+D+E+(1|H)+(B|H), where A is distance between electrodes (mm), B is stimulation level (μA), C and D are stimulation and response channel tissue types, respectively, E is the categorical variable of stimulation/response in the SOZ, F is the CCEP amplitude (μV) that was log-transformed, and H represents patient identity. Post-hoc statistical comparisons within factors were made using an omnibus Kruskal-Wallis (KW) test at the factor level and then proceeding with pairwise comparisons using rank-sum tests that were corrected for multiple comparisons using the Tukey-Kramer method ($p<0.05$).

A similar procedure was used to analyze gamma power as the dependent variable. Parameter estimation was done using a maximum pseudolikelihood method using the MATLAB function fitglme. Data from all patients from the standard and high-resolution mapping were combined in this model. The same model was repeated, with F representing the log-transformed evoked gamma-band power. Gamma power skewed positively (Lilliefors test, kstat=0.44, p=0.001, critical value=0.0023) visually and was corrected with log-transformation (Lilliefors test, kstat=0.05, p=0.001, critical value=0.0023). Post-hoc statistical comparisons were completed as described above.

Results

Of the 11 recruited patients (Table 1), 7 received “standard” stimulation mapping and 6 received “high-resolution” mapping; 2 received both protocols. There were 156,935 total responses. CCEPs were detected in 4,370 stimulation-response pairs across all patients: 4,218 in the “standard” and 265 in the “high-resolution” group with some overlap.

An example response is shown in Figure 1A. After SPES was applied to an electrode, the largest CCEPs were seen on nearby electrodes, with nonuniform spread to the left anterior and posterior hippocampus. Single-trial CCEPs during SPES of the same electrodes are shown at four stimulation intensities (Figure 1B). See Supplementary Figure 2 for an example of grid-derived CCEPs from patient 2. To define predictors of CCEP amplitude, a linear mixed-effects model was fit to this dataset across patients. Total adjusted R^2=0.36 in the model indicated that 36% of the variability in CCEP amplitude was explained by the model’s fixed effects.

CCEP amplitude varies by stimulation level

Twenty stimulation levels were used in the model (0.5-10.0 mA). Increasing stimulation level by 1 mA increased the CCEP amplitude by 3% (Figure 2A,B, Table 2). Interlevel variability was greatest at lower stimulation levels (i.e., greater variation in response amplitude at 2.5 than 5.0 mA) (Figures 1B, 2A,B). Post-hoc pairwise comparison within the “standard” mapping dataset showed a significant difference in CCEP amplitude at 2.5 mA versus all other stimulation amplitudes (pairwise rank-sum tests, $p<0.05$) and at 5.0 versus 7.5 and 10.0 mA, but not between 7.5 and 10.0 mA.

Post-hoc pairwise comparison using the “high-resolution” mapping group showed CCEP amplitude plateaued after ~5.5 mA. There was no significant difference between CCEPs at

levels ≥5.5 mA (pairwise rank-sum tests, p<0.05, Figure 2B). Overall, stimulation at ≥5.5 mA yielded a reliable and maximal CCEP across stimulation-response pairs over all regions.

CCEP amplitude varies by distance

Increasing stimulation-response electrode distance by 1 mm predicted that CCEP amplitude decreased by 2.9%. Responses were measured from 2.4 to 108.0 mm (mean 17.3 mm). Greater distances between electrodes were related to smaller CCEP amplitude out to ~50 mm, after which there was a relative asymptote (Figure 3A,B, Table 2). Subanalysis showed that greater stimulation intensity was required to generate a CCEP at greater distances (Figure 3C). A KW test showed the main effect of spatial spread for the "standard" (χ^2=178, df=3, p=3*10^{-38}) and "high-resolution" (χ^2=120, df=19, p=9.77*10^{-17}) stimulation datasets. Follow-up pairwise comparisons are shown in Figure 3C. For the "high-resolution" dataset, we could not detect differences in spread from ≥3.5 mA by post-hoc pairwise comparison (Figure 3D, rank-sum tests, p<0.05, Tukey-Kramer corrected). Stimulation below 1.5-mA monopolar configuration creates CCEPs only locally within 0.5 cm on average.

CCEP waveform shape varies by stimulation level

Waveform shape changed significantly across stimulation amplitudes (KW test for "standard" [χ^2=5.25*10^3, df=5, p=0] and "high-resolution" [χ^2=1.01*10^4, df=189, p=0] stimulation). As expected, waveform shapes had higher correlation coefficients at similar stimulation levels. For example, stimulation at 9.5 and 10.0 mA produced similar waveforms (Figure 4A, pairwise rank-sum test, p<0.05, Tukey-Kramer corrected), whereas stimulation at 3.5 and 10.0 mA produced waveforms of dissimilar shape (Figure 4B). Importantly, there was greater variability at lower stimulation intensities than at high stimulation intensities (Figure 4C,D). For example, the correlation between 2.5 and 5.0 mA was lower than that between 5.0 and 10.0 mA, although both comparisons had a twofold increase in stimulation intensity. Comparisons across all stimulation levels are reported in Figure 4C–F.

CCEP amplitude varies by anatomical location

Using the generalized linear mixed-effects model, the location of both the stimulation (Figure 5A, Table 2; KW test, χ^2=451, df=3, p=1.62*10^{-97}) and the response (Figure 5B, Table 2; KW test, χ^2=1.30*10^3, df=3, p=2.25*10^{-282}) electrodes had a significant effect on CCEP amplitude, with post-hoc testing showing that the responses in all areas were different from each other (p<0.05, Tukey-Kramer corrected, Figure 5B). The hippocampus generated the largest CCEP whether it was the location of the stimulation (Figure 5A) or the response (Figure 5B) electrode. Note that subdural contacts exclusively stimulate gray matter based on their anatomical location/orientation. SEEG electrodes may be in contact with white or gray matter. We determined those contacts in white matter based on imaging and for completeness we ran the model without white matter stimulation trials and found no qualitative differences in the results (Supplementary table 1).

CCEP amplitude is larger within the SOZ

A single categorical variable in the model represented whether the stimulation electrode, response electrode, or both were in the SOZ. The SOZ was defined based on documented ictal onsets during long-term intracranial monitoring. There were some cases where the clinical SOZ was determined to be larger than this, based on clinical factors or interictal activity (as in patient 7, with clinically diagnosed bitemporal epilepsy, but seizures only recorded from the left hippocampus). In all cases, we conservatively only labeled electrode contacts as part of the SOZ if the epileptologist documented ictal onset from that contact. Patients 5, 8, and 10 had regional/multifocal onset epilepsy with no definitively identified SOZ (Table 1). We therefore did not label any contacts as part of the SOZ for those patients. Patient 7 had documented ictal onset from the left hippocampus, but frequent interictal activity from the right hippocampus.

Because of this picture, the patient was clinically determined to have bitemporal epilepsy. However, since we could only prove for certain left-sided involvement, we only labeled these contacts as part of the SOZ. Using this convention the CCEP was 9.9% larger if either stimulation electrode, response electrode or both were in the SOZ (Figure 6A, Table 2). In the case where there was bitemporal SOZ foci as in patients 1, 3, and 6, we compared the CCEP amplitude between sides and found there to be a difference between left and right sides across patients (all $p<0.001$).

Evoked gamma-band power is associated with changes in stimulation level, anatomical location, and the SOZ

We fit the same linear mixed-effects model to the log-transformed evoked gamma-band power as the dependent variable and found similar results to the CCEP amplitude analysis above. The total adjusted $R^2=0.52$ indicated that 52% of the variability in the evoked gamma amplitude was explained by the model's fixed effects. The gamma waveform shape is shown in Figure 1B.

Increases in stimulation level of 1 mA evoked 3% greater evoked gamma-band power across electrode locations (Table 3). The evoked gamma-band power in the "standard" stimulation configuration plateaued beyond 7.5-mA stimulation (Figure 2C). This trend was also reflected in the "high-resolution" dataset, but the plateau occurred at 5.0-mA stimulation (Figure 2D). There was a main effect of distance on evoked gamma-band power based on the model (Figure 3B, Table 3). Inspection of the raw data shows there was a peak at 3.0 cm and then a relative asymptote above 4.0 cm distance (Figure 3B).

Stimulation location significantly affected evoked gamma-band power (Table 3). Interestingly, stimulation of the amygdala yielded the largest evoked gamma-band power across all response areas (KW test, $\chi^2=5.42*10^3$, df=3, $p=0$; all significant pairwise comparisons, rank-sum tests, $p<0.05$, Tukey-Kramer corrected, Figure 5C). Stimulation of the hippocampus generated the second largest gamma-band response and had a significantly different mean compared with all other response areas. As with CCEP amplitude, response region also significantly affected evoked gamma-band power (Figure 5D, Table 3; KW test, $\chi^2=6.10*10^3$, df=3, $p=0$). Pairwise comparisons showed the largest gamma-band response

was evoked within the hippocampus (pairwise rank-sum tests, $p<0.05$, Tukey-Kramer corrected). Significant differences were also observed in the amygdala and neocortex. Note that for completeness we ran the model without white matter stimulation trials and found no qualitative differences in the results (Supplementary table 2).

Finally, evoked gamma-band power was 120.0% larger when the stimulation contact or the response contact or both were in the SOZ (Figure 6B, Table 3). In the case where there was bitemporal SOZ foci as in patients 1, 3, and 6, we compared the evoked gamma band power between sides and found there to be a difference between left and right sides across patients (all $p<0.001$, Supplementary Figure 3).

Discussion

CCEPs are a reliable measure of effective connectivity but are highly variable across patients and stimulation paradigms. Through rigorous statistical analysis of a large dataset (156,935 responses), we showed that much of this variability is explained by a model incorporating anatomical location, stimulation amplitude, and stimulation-response distance. Critically, we were able to generalize these results across patients by accounting for patient as a source of random variance.

From an anatomical perspective, we showed that there were different evoked responses in different tissue types, namely hippocampus versus amygdala versus neocortex. For the first time, we report that the hippocampus consistently showed the largest CCEPs as either the stimulation or the response electrode (Figure 5A,B). The hippocampus also showed the largest evoked gamma response, specifically as the response electrode. We also provided a unique comparison of how CCEP amplitude and evoked gamma-band power, another unique measure of cortical activation, may change differentially with stimulation parameter changes. Finally, we showed that gamma power (70-150 Hz) was larger in the SOZ compared with outside the SOZ across patients, reinforcing results from prior studies [22,27–29]. The clinical implications of these findings and related literature are discussed below.

Different components of the CCEP waveform (N1 and N2) have been related to stimulation parameters, such as stimulation current, as well as response location, particularly if within the SOZ versus normal brain [6,30,31]. We found a significant relationship between stimulation current and the CCEP amplitude, which has been shown to be related ultimately to the charge per phase delivered to the tissue [17,32]. An upper bound of stimulation has not been delineated beyond that of possible tissue damage from excessive charge per phase with high frequency stimulation experiments [33]. In contrast, we characterize a nonlinearity in the relationship between stimulation current and CCEP amplitude whereby a plateau is apparent with monopolar stimulation at 5.5-7.5 mA (cutoff varied between “standard” and “high-resolution” stimulation protocols likely due to the number of patients in the groups used to capture the transition zone, Figure 2). Beyond these stimulation currents/levels, no further significant increase in CCEP amplitude could be detected. An explanation for the nonlinearity may be that the current flux experienced from a point source is proportional to the current amplitude of the source and inversely related to the distance from the source and

to the conductivity of the medium [34]. Thus, increasing the current may recruit more tissue to reach threshold at a certain distance. Modeling and experimental data show that the voltage "seen" by an electrode is related to an exponential decay as a function of the distance from stimulation ($V \sim 1/r^x$) [35,36], where x determines the location of the asymptote of the curvature of the voltage as a function of distance. Thus, the asymptotic threshold we find at 5.5-mA current amplitude may be the point at which effectively the entire volume of "activatable" tissue (i.e., all neuronal ensembles near the stimulation channel and all distant neuronal ensembles that are in the stimulation-response pair network) is being activated. Additionally, with cathodic monopolar stimulation of an axon, flanking areas of depolarization are areas of hyperpolarization or "virtual anodes" that would influence the activation threshold [37] and may cause the CCEP amplitude to plateau.

Reaching asymptotic threshold may be critical for downstream analyses with single-pulse stimulation. For example, in a prior study, we stimulated at 3.5-mA biphasic pulses to identify features of the SOZ [38]. We were able to predict the location of the SOZ in 6/10 patients but were unable to obtain reliable CCEPs in some patients for whom we were subsequently unable to predict the location of the SOZ. Other studies have found a mixed relationship between CCEP features or evoked gamma power and the location of the SOZ but stimulated with current levels of ≤5 mA [22,39,40], which may not have reached the threshold necessary to obtain reliable responses.

We found that waveform shape evolved with increasing stimulation intensity. Event-related potential (ERP) theory posits that components (i.e., the negative- and positive-going peaks) of the ERP are related to anatomically and/or functionally distinct neuronal ensembles or networks underlying that task or brain state [41]. It follows that larger stimulation intensities may recruit more such functional ensembles, which give rise to additional components of the CCEP waveform. Our data corroborate these observations (Figures 1, 2, 4B). Higher stimulation levels evoked a more reliable waveform with more complex features, which may reflect distinct neural components (Figure 4).

We found a relationship between stimulation intensity and evoked gamma-band response amplitude whereby increases in the former resulted in an increase in the latter across stimulation response-channel pairs. There appears to be a threshold stimulation current of 5.5-7.5 mA, depending on stimulation protocol, beyond which the evoked gamma amplitude does not increase (Figure 2C,D). Similarly, Crowther et al. used a smaller distribution of neocortical regions to show a correlation between evoked gamma power of 70-170 Hz and stimulation current adjusted from 4 to 15 mA [14]. There was no difference between gamma amplitude from medium-current (8-10 mA) and high-current (15 mA) stimulation groups, but both those groups were larger than the low (4-6 mA)-stimulation group. These results support the threshold effect reported here for both gamma-band power and CCEP amplitude.

We found CCEP amplitude decreased with distance, consistent with prior studies [6,39,42]. Biophysical factors contributing to this trend likely reflect the divergence of stimulating fiber tracts as they leave the stimulated region. Obtaining a CCEP at greater distances required larger stimulation currents up to the qualitative plateau at 5.5 mA. Interestingly, the evoked gamma response differed from the CCEP responses in that it had a peak in the

evoked power at a distance of 2-3.5 cm from the stimulating electrode (Figure 3B) whereas the CCEP amplitude showed a steady fall-off with distance (Figure 3A). This effect may be related to activation of cortical neuronal populations (which may be more clinically relevant) versus measuring the slow potentials associated with postsynaptic activity (i.e., the raw CCEP), although the physiological basis for gamma-band power and ERPs is controversial and depends on the electrode type by which the signal is measured [43,44]. Of note, distant contralateral CCEPs can be seen in patients with stimulation ipsilaterally (Supplementary Figure 4) and see [39]. This may be related to unique axonal connectivity across the cerebral hemispheres. There may also be large responses from stimulation of temporal lobe to evoked responses in the frontal lobe, following the language network for example [8]. Unfortunately, our linear model would not capture this type of distant amplification relationship between lobes or across the cerebrum as the vast majority of responses are local to stimulation and fall off with short distances.

The hippocampus consistently showed the largest CCEPs whether it was the stimulation or response electrode (Figure 5A,B) and also showed the largest evoked gamma response, specifically as the response electrode (Figure 5D). To our knowledge, these results have not been described previously in humans. Large or “giant” CCEP responses up to 1mV in amplitude have been documented in mesial temporal lobe structures in the literature [45,46]. The physiological basis may be that both the hippocampus and amygdala have extensive connectivity with neocortical areas as was shown with CCEPs derived from stimulation of these structures [47]. The largest CCEPs we noted were around 2 mV. Interestingly, stimulation of the amygdala resulted in the largest evoked gamma responses across brain regions. This result is supported by the results of Enatsu et al., who showed greater outgoing connectivity from amygdala to limbic as well as extralimbic areas compared with hippocampus [48].

The most clinically relevant finding from this study was that the “early” period CCEP amplitude was 9.9% larger and the evoked gamma band response was 120.0% larger in the SOZ compared to the non-SOZ contacts. Importantly, because we used a multivariable regression model, these results are taking into account the variance related to stimulation amplitude, channel location, and even the random variance related to patient, thus the quantification can be generalized across patients and those other factors. These results follow prior literature in field. The earliest data showed that the occurrence of “delayed” (100-1000 ms poststimulation) CCEP components are more frequent in the SOZ of patients with neocortical epilepsy [22,49]. In later studies, the components of the CCEP were measured and the SOZ location was found to be related to the CCEP amplitude (amplitude of the N1 peak [30]) and evoked gamma response [29,50]. We focused on the “early” time period (0-100 ms) [29–31], but others have also looked at a “delayed” period [22,27,28,50]. We found that the responses in the SOZ were larger for both the CCEP amplitude and evoked gamma response (Figure 6 A,B). Prior to us, Mouthaan et al looked at a similar band (>80 Hz) during the early period and found the rate of visually-determined responses to be higher in the SOZ versus outside the SOZ for 3 of 5 patients [29]. Kobayashi et al further explored this effect and found that subdural channels with higher power in the ripple (<200 Hz) and fast ripple (>200 Hz) frequency bands during the N1 peak (<50 ms post-stimulation) were associated with the SOZ location [31]. The vast majority of these studies

in the literature include focal onset epilepsy patients whom had foci in the mesial temporal lobe or outside that region. Several of our study patients have regional/multifocal seizure onset, and in those cases, we did not label any particular contacts as part of the seizure focus. It may be that for those patients, we are "missing" the clinical SOZ. To address this, we recreated our models without the data from our regional/multifocal onset patients to look at how potentially "mislabeling or missing" the SOZ would affect the model results. This improved both models. As expected, (if we assume CCEP amplitude and evoked gamma power are markers of the SOZ), the effect of SOZ as a factor in predicting CCEP amplitude and evoked gamma power increased. CCEP amplitude increases 10.6% (vs 9.9% including those patients) and gamma power increases 127.4% (vs 120.0% including those patients) for contacts in the SOZ across patients (data not included). In other words, those regional onset epilepsy patients may have SOZ channels which we were not able to discern clinically. There were no other qualitative changes in the model results.

Importantly, our automated stimulation protocol can easily be incorporated into a clinical mapping protocol for isolating the SOZ, see review by Matsumoto et al describing this work [6]. Prior protocols require visual assessment of waveforms which can be time consuming [30,49,50]. The CCEP amplitude and evoked gamma band power measurements can be added into a clinician's folio of SOZ mapping data including results from nuclear imaging, intracranial monitoring, and ictal mapping using high frequency stimulation. More data will be needed to establish normative values for CCEP-based measurements within the SOZ and non-SOZ tissue across patients. Data from this study provides some of the first benchmarks for this. The hope is to identify a set of features of the CCEP with high enough sensitivity and specificity that long term monitoring data will not be required to find the SOZ.

Additionally, epilepsy is increasingly being viewed as a disease of a network [2,51,52]. The prevailing theory still being that there is an imbalance of excitation and inhibition either between cells of a node or multiple nodes, resulting in seizure generation and propagation. CCEPs can be used not only to probe the epileptogenicity of a focus as described above, but also to probe the seizure network [6]. Direct anatomical connectivity can be parsed with CCEP analysis [8,9,53]. These underlying networks themselves may explain seizure propagation for certain types of focal epilepsy, see [6] for examples and discussion. Recent investigations have also characterized how high frequency pulsed stimulation during ictal activity changes that activity and predicts the responsiveness of a patient to responsive neurostimulation treatment [54]. This illustrates a continuum of research investigating the effects of brain stimulation and how stimulation can further inform regarding the nature of an epileptogenic network. CCEP propagation has been directly related to measures of structural connectivity [4,55] and functional connectivity [56]. We hope to incorporate tractography based measures into future studies to model the CCEP response. Data shows that in patients with epilepsy, there is increased resting-state functional connectivity within the epileptogenic zone but decreased connectivity within other functional networks such as the default mode [51,52,57]. Improved functional connectivity in the ascending reticular activating system is related to better rates of seizure freedom postoperatively [58]. Future CCEP-based studies may bolster these findings.

There are several limitations to this study. Each electrode pair was stimulated 10 times, limiting the reliability of the trial average CCEP estimate. Additionally, accuracy of coregistration between the preoperative MRI and postoperative CT is limited, which may lead to misclassification of the electrode location. The mixed-effects model captures multivariable data, controlling for random variance, but practical computing limitations limit the number of interaction effects we can assess. We assume the system behaves as a linear time-invariant system in the model; however, nonlinearities are likely to exist and higher-order terms may be explored in the future with larger datasets. Finally, we delivered stimulation in a monopolar fashion, which we believe makes it easier to attribute responses to precise stimulation locations, but most previous studies delivered bipolar stimulation [8,9,27]. Finally, direct translation of these results to the effects of high frequency stimulation used in neuromodulation modalities such as deep brain stimulation or the closed-loop technology of responsive neurostimulation cannot be made from the data this study. However, efforts to characterize plasticity related to high frequency stimulation using CCEP-based measures of effective connectivity are underway [59]. Such studies will help inform how high frequency stimulation paradigms work. High frequency stimulation (generally above 50 Hz) was originally thought to be related to a lesion effect. It is increasingly being recognized that the effects of high frequency stimulation are related to complex modulation of a network that varies its effects with location of stimulation and proximity to fiber tracts [60,61]. Finally, in direct clinical application, recent data derived from epilepsy patients implanted with the responsive neurostimulation device shows high frequency pulsed stimulation during ictal activity modulates that activity and that modulation pattern may predict the responsiveness of a patient to responsive neurostimulation treatment [54].

Conclusion

In this study, we characterize the responses from SPES across a range of stimulation parameters and brain regions and provide data to support guidelines for reliable stimulation parameters in epilepsy patients. We found that stimulation levels above 5.5-7.5 mA will not generate higher CCEPs across brain areas, and stimulation levels below 5.5-7.5 mA generate more variable responses. Thus, 5.5-7.5 mA may be an asymptotic threshold to consider for SPES analyses using monopolar stimulation. Evoked gamma-band power exhibited a similar asymptotic current threshold. Amplitudes of both measures fall off with distance, although gamma-band power exhibited a peak at 2.0-3.5 cm distance between stimulation and response measurement contacts. We show that the location of the clinical SOZ has larger CCEP amplitude and evoked gamma power responses, and for the first time, we show that CCEPs and evoked gamma power are larger when measured in the hippocampus than in most other cortical brain areas.

Supplementary Material

Refer to Web version on PubMed Central for supplementary material.

Acknowledgments

We would like to thank Kristin Kraus for her editorial comments.

Funding: JDR is supported by the NIH, NCATS KL2 TR002539 and NINDS R21 NS113031. BK is supported in part by a NREF neurosurgical research grant.

Abbreviations:

CCEP	corticocortical evoked potential
SPES	single-pulse electrical stimulation
SOZ	seizure onset zone
SEEG	stereotactic electroencephalography
fMRI	functional magnetic resonance imaging

References

[1]. Bressler SL, Menon V. Large-scale brain networks in cognition: emerging methods and principles. Trends Cogn Sci 2010;14:277–90. doi:10.1016/j.tics.2010.04.004. [PubMed: 20493761]

[2]. Smith EH, Schevon CA. Toward a Mechanistic Understanding of Epileptic Networks. Curr Neurol Neurosci Rep 2016;16. doi:10.1007/s11910-016-0701-2. [PubMed: 26753870]

[3]. Smith EH, Liou J- Y, Davis TS, Merricks EM, Kellis SS, Weiss SA, et al. The ictal wavefront is the spatiotemporal source of discharges during spontaneous human seizures. Nat Commun 2016;7:11098. doi:10.1038/ncomms11098. [PubMed: 27020798]

[4]. Keller CJ, Honey CJ, Megevand P, Entz L, Ulbert I, Mehta AD, et al. Mapping human brain networks with cortico-cortical evoked potentials. Philos Trans R Soc B Biol Sci 2014;369:20130528-. doi:10.1098/rstb.2013.0528.

[5]. Prime D, Rowlands D, O'Keefe S, Dionisio S. Considerations in performing and analyzing the responses of cortico-cortical evoked potentials in stereo-EEG. Epilepsia 2018;59:16–26. doi:10.1111/epi.13939. [PubMed: 29143307]

[6]. Matsumoto R, Kunieda T, Nair D. Single pulse electrical stimulation to probe functional and pathological connectivity in epilepsy. Seizure 2017;44:27–36. doi: 10.1016/j.seizure.2016.11.003. [PubMed: 27939100]

[7]. Friston KJ. Functional and Effective Connectivity in Neuroimaging: A synthesis. Hum Brain Mapp 1994;2:56–78.

[8]. Matsumoto R, Nair DR, LaPresto E, Najm I, Bingaman W, Shibasaki H, et al. Functional connectivity in the human language system: A cortico-cortical evoked potential study. Brain 2004;127:2316–30. doi:10.1093/brain/awh246. [PubMed: 15269116]

[9]. Matsumoto R, Nair DR, LaPresto E, Bingaman W, Shibasaki H, Lüers HO. Functional connectivity in human cortical motor system: A cortico-cortical evoked potential study. Brain 2007;130:181–97. doi:10.1093/brain/awl257. [PubMed: 17046857]

[10]. Parker CS, Clayden JD, Cardoso MJ, Rodionov R, Duncan JS, Scott C, et al. Structural and effective connectivity in focal epilepsy. Neuroimage Clin 2018;17:943–52. doi:10.1016/j.nicl.2017.12.020. [PubMed: 29527498]

[11]. Usami K, Matsumoto R, Kobayashi K, Hitomi T, Matsuhashi M, Shimotake A, et al. Phasic REM Transiently Approaches Wakefulness in the Human Cortex-A Single-Pulse Electrical Stimulation Study. Sleep 2017;40. doi:10.1093/sleep/zsx077.

[12]. Matsumoto R, Nair DR, Ikeda A, Fumuro T, Lapresto E, Mikuni N, et al. Parieto-frontal network in humans studied by cortico-cortical evoked potential. Hum Brain Mapp 2012;33:2856–72. doi:10.1002/hbm.21407. [PubMed: 21928311]

[13]. Basu I, Robertson MM, Crocker B, Peled N, Farnes K, Vallejo-Lopez DI, et al. Consistent Linear and Non-Linear Responses to Invasive Electrical Brain Stimulation Across Individuals and Primate Species with Implanted Electrodes. Brain Stimul 2019. doi:10.1016/j.brs.2019.03.007.

[14]. Crowther LJ, Brunner P, Kapeller C, Guger C, Kamada K, Bunch ME, et al. A quantitative method for evaluating cortical responses to electrical stimulation. J Neurosci Methods 2019. doi:10.1016/j.jneumeth.2018.09.034.

[15]. Nathan SS, Sinha SR, Gordon B, Lesser RP, Thakor N V. Determination of current density distributions generated by electrical stimulation of the human cerebral cortex. Electroencephalogr Clin Neurophysiol 1993;86:183–92. doi:10.1016/0013-4694(93)90006-H. [PubMed: 7680994]

[16]. Abou-Al-Shaar H, Brock AA, Kundu B, Englot DJ, Rolston JD. Increased nationwide use of stereoencephalography for intracranial epilepsy electroencephalography recordings. J Clin Neurosci 2018. doi:10.1016/j.jocn.2018.04.064.

[17]. Donos C, Mîndruţă I, Ciurea J, Mălîia MD, Barborica A. A comparative study of the effects of pulse parameters for intracranial direct electrical stimulation in epilepsy. Clin Neurophysiol 2016;127:91–101. doi:10.1016/j.clinph.2015.02.013. [PubMed: 25910851]

[18]. Keller CJ, Mégevand P, Mehta AD, Honey CJ, Entz L, Ulbert I. Mapping human brain networks with cortico-ortical evoked potentials. Philos Trans R Soc B Biol Sci 2014;369. doi: 10.1098/rstb.2013.0528.

[19]. Crone N, Miglioretti DL, Gordon B, Lesser RP. Functional mapping of human sensorimotor cortex with electrocorticographic spectral analysis. Brain 1998;121:2301–15. doi:10.1093/brain/121.12.2301. [PubMed: 9874481]

[20]. Lega B, Dionisio S, Flanigan P, Bingaman W, Najm I, Nair D, et al. Cortico-cortical evoked potentials for sites of early versus late seizure spread in stereoelectroencephalography. Epilepsy Res 2015;115:17–29. doi: 10.1016/j.eplepsyres.2015.04.009. [PubMed: 26220373]

[21]. Anderson DN, Duffley G, Vorwerk J, Dorval AD, Butson CR. Anodic stimulation misunderstood: Preferential activation of fiber orientations with anodic waveforms in deep brain stimulation. J Neural Eng 2019;16. doi:10.1088/1741-2552/aae590.

[22]. Valentín A, Anderson M, Alarcón G, Seoane JJG, Selway R, Binnie CD, et al. Responses to single pulse electrical stimulation identify epileptogenesis in the human brain in vivo. Brain 2002;125:1709–18. [PubMed: 12135963]

[23]. Conner C, Ellmore TM, DiSano MA, Pieters TA, Potter AW, Tandon N. Anatomic and electro-physiologic connectivity of the language system: A combined DTI-CCEP study. Comput Biol Med 2011;41:1100–9. doi:10.1016/j.compbiomed.2011.07.008. [PubMed: 21851933]

[24]. Rolston JD, Gross RE, Potter SM. Common median referencing for improved action potential detection with multielectrode arrays. Proc 31st Annu Int Conf IEEE Eng Med Biol Soc Eng Futur Biomed EMBC 2009 2009:1604–7. doi:10.1109/IEMBS.2009.5333230.

[25]. Rolston JD, Laxpati NG, Gutekunst CA, Potter SM, Gross RE. Spontaneous and evoked high-frequency oscillations in the tetanus toxin model of epilepsy. Epilepsia 2010;51:2289–96. doi:10.1111/j.1528-1167.2010.02753.x. [PubMed: 20946126]

[26]. Lilliefors HW. On the Kolmogorov-Smirnov Test for Normality with Mean and Variance Unknown. vol. 62 1967.

[27]. Valentín A, Alarcón G, Honavar M, García Seoane JJ, Selway RP, Polkey CE, et al. Single pulse electrical stimulation for identification of structural abnormalities and prediction of seizure outcome after epilepsy surgery: A prospective study. Lancet Neurol 2005. doi:10.1016/S1474-4422(05)70200-3.

[28]. Flanagan D, Valentín A, García Seoane JJ, Alarcón G, Boyd SG. Single-pulse electrical stimulation helps to identify epileptogenic cortex in children. Epilepsia 2009;50:1793–803. doi:10.1111/j.1528-1167.2009.02056.x. [PubMed: 19453705]

[29]. Mouthaan BE, Van't Klooster MA, Keizer D, Hebbink GJ, Leijten FSS, Ferrier CH, et al. Single Pulse Electrical Stimulation to identify epileptogenic cortex: Clinical information obtained from early evoked responses. Clin Neurophysiol 2016;127:1088–98. doi:10.1016/j.clinph.2015.07.031. [PubMed: 26377063]

[30]. Iwasaki M, Enatsu R, Matsumoto R, Novak E, Thankappen B, Piao Z, et al. Accentuated cortico-cortical evoked potentials in neocortical epilepsy in areas of ictal onset. Epileptic Disord 2010;12:292–302. [PubMed: 20952353]

[31]. Kobayashi K, Matsumoto R, Matsuhashi M, Usami K, Shimotake A, Kunieda T, et al. High frequency activity overriding cortico-cortical evoked potentials reflects altered excitability in the

human epileptic focus. Clin Neurophysiol 2017;128:1673–81. doi: 10.1016/j.clinph.2017.06.249. [PubMed: 28750290]

[32]. Rutecki PA, Grossman RG, Armstrong D, Irish-Loewen S. Electrophysiological connections between the hippocampus and entorhinal cortex in patients with complex partial seizures. J Neurosurg 2009;70:667–75. doi:10.3171/jns.1989.70.5.0667.

[33]. McIntyre CC, Grill WM. Finite element analysis of the current-density and electric field generated by metal microelectrodes. Ann Biomed Eng 2001;29:227–35. doi: 10.1114/1.1352640. [PubMed: 11310784]

[34]. Malmivuo J, Plonsey R. Chapter 8: Source Field Models. Bioelectromagn. Princ. Appl. Bioelectric Biomagn. Fields, 1995.

[35]. Miocinovic S, Lempka SF, Russo G, Maks C, Butson C, Sakaie KE, et al. Experimental and theoretical characterization of the voltage distribution generated by deep brain stimulation. Exp Neurol 2009;216:166–76. doi:10.1371/journal.pone.0178059. [PubMed: 19118551]

[36]. Butson C, McIntyre CC. Role of electrode design on the volume of tissue activated during deep brain stimulation. J Neural Eng 2006;3:1–8. doi:10.1038/jid.2014.371. [PubMed: 16510937]

[37]. Brocker D, Grill W. Chapter 1: Principles of electrical stimulation of neural tissue In: Lozano A, Hallett M, editors. Brain Stimul. Handb. Clin. Neurol. Vol 116, Amsterdam: Elsevier B.V.; 2013, p. 3–18.

[38]. Davis TS, Rolston JD, Bollo RJ, House PA. Delayed high-frequency suppression after automated single-pulse electrical stimulation identifies the seizure onset zone in patients with refractory epilepsy. Clin Neurophysiol 2018. doi:10.1016/j.clinph.2018.06.021.

[39]. Lacruz ME, García Seoane JJ, Valentin A, Selway R, Alarcón G. Frontal and temporal functional connections of the living human brain. Eur J Neurosci 2007;26:1357–70. doi:10.1111/j.1460-9568.2007.05730.x. [PubMed: 17767512]

[40]. Maliia MD, Donos C, Barborica A, Mindruta I, Popa I, Ene M, et al. High frequency spectral changes induced by single-pulse electric stimulation: Comparison between physiologic and pathologic networks. Clin Neurophysiol 2017;128:1053–60. doi:10.1016/j.clinph.2016.12.016. [PubMed: 28131532]

[41]. Luck SJ (Steven J. An introduction to the event-related potential technique. n.d.

[42]. Kunieda T, Yamao Y, Kikuchi T, Matsumoto R. New approach for exploring cerebral functional connectivity: Review of cortico-cortical evoked potential. Neurol Med Chir (Tokyo) 2015;55:374–82. doi:10.2176/nmc.ra.2014-0388. [PubMed: 25925755]

[43]. Watson BO, Ding M, Buzsáki G. Temporal coupling of field potentials and action potentials in the neocortex. Eur J Neurosci 2018:1–16. doi:10.1111/ejn.13807.

[44]. Manning JR, Jacobs J, Fried I, Kahana MJ. Broadband shifts in local field potential power spectra are correlated with single-neuron spiking in humans. J Neurosci 2009;29:13613–20. doi:10.1523/JNEUR0SCI.2041-09.2009. [PubMed: 19864573]

[45]. Wilson CL, Khan SU, Engel J, Isokawa M, Babb TL, Behnke EJ. Paired pulsed suppression and facilitation in human epileptogenic hippocampal formation. Epilepsy Res 1998;31:211–30. doi:10.1016/S0920-1211(98)00063-1. [PubMed: 9722031]

[46]. Takeyama H, Matsumoto R, Usami K, Nakae T, Kobayashi K, Shimotake A, et al. Human entorhinal cortex electrical stimulation evoked short-latency potentials in the broad neocortical regions: Evidence from cortico-cortical evoked potential recordings. Brain Behav 2019;9:1–13. doi:10.1002/brb3.1366.

[47]. Mégevand P, Groppe DM, Bickel S, Mercier MR, Goldfinger MS, Keller CJ, et al. The Hippocampus and Amygdala Are Integrators of Neocortical Influence: A CorticoCortical Evoked Potential Study. Brain Connect 2017;7:648–60. doi:10.1089/brain.2017.0527. [PubMed: 28978234]

[48]. Enatsu R, Gonzalez-Martinez J, Bulacio J, Kubota Y, Mosher J, Burgess RC, et al. Connections of the limbic network: A corticocortical evoked potentials study. Cortex 2015. doi:10.1016/j.cortex.2014.06.018.

[49]. Valentín A, Alarcón G, Honavar M, García Seoane JJ, Selway RP, Polkey CE, et al. Single pulse electrical stimulation for identification of structural abnormalities and prediction of seizure

outcome after epilepsy surgery: A prospective study. Lancet Neurol 2005;4:718–26. doi:10.1016/S1474-4422(05)70200-3. [PubMed: 16239178]

[50]. Van'T Klooster MA, Zijlmans M, Leijten FSS, Ferrier CH, Van Putten MJAM, Huiskamp GJM. Time-frequency analysis of single pulse electrical stimulation to assist delineation of epileptogenic cortex. Brain 2011;134:2855–66. doi:10.1093/brain/awr211. [PubMed: 21900209]

[51]. Englot DJ, Konrad PE, Morgan VL. Regional and global connectivity disturbances in focal epilepsy, related neurocognitive sequelae, and potential mechanistic underpinnings. Epilepsia 2016;57:1546–57. doi:10.1111/epi.13510. [PubMed: 27554793]

[52]. Englot DJ, Gonzalez HFJ, Reynolds BB, Konrad PE, Jacobs ML, Gore JC, et al. Relating structural and functional brainstem connectivity to disease measures in epilepsy. Neurology 2018;91:E67–77. doi:10.1212/WNL.0000000000005733. [PubMed: 29848786]

[53]. Enatsu R, Gonzalez-Martinez J, Bulacio J, Kubota Y, Mosher J, Burgess RC, et al. Connections of the limbic network: A corticocortical evoked potentials study. Cortex 2015;62:20–33. doi:10.1016/j.cortex.2014.06.018. [PubMed: 25131616]

[54]. Kokkinos V, Sisterson ND, Wozny TA, Richardson RM. Association of Closed-Loop Brain Stimulation Neurophysiological Features with Seizure Control among Patients with Focal Epilepsy. JAMA Neurol 2019;76:800–8. doi:10.1001/jamaneurol.2019.0658. [PubMed: 30985902]

[55]. Keller CJ, Honey CJ, Entz L, Bickel S, Groppe DM, Toth E, et al. Corticocortical evoked potentials reveal projectors and integrators in human brain networks. J Neurosci 2014;34:9152–63. doi:10.1523/JNEUROSCI.4289-13.2014. [PubMed: 24990935]

[56]. Keller CJ, Bickel S, Entz L, Ulbert I, Milham MP, Kelly C, et al. Intrinsic functional architecture predicts electrically evoked responses in the human brain. Proc Natl Acad Sci 2011;108:10308–13. doi:10.1073/pnas.1019750108. [PubMed: 21636787]

[57]. Englot DJ, Hinkley LB, Kort NS, Imber BS, Mizuiri D, Honma SM, et al. Global and regional functional connectivity maps of neural oscillations in focal epilepsy. Brain 2015;138:2249–62. doi:10.1093/brain/awv130. [PubMed: 25981965]

[58]. González HFJ, Goodale SE, Jacobs ML, Haas KF, Landman BA, Morgan VL, et al. Brainstem Functional Connectivity Disturbances in Epilepsy may Recover After Successful Surgery. Neurosurgery 2019. doi:10.1093/neuros/nyz128.

[59]. Huang Y, Hajnal B, Entz L, Fabó D, Herrero JL, Mehta AD, et al. Intracortical Dynamics Underlying Repetitive Stimulation Predicts Changes in Network Connectivity. J Neurosci 2019;39:6122–35. doi:10.1523/JNEUROSCI.0535-19.2019. [PubMed: 31182638]

[60]. Ramirez-Zamora A, Giordano J, Boyden ES, Gradinaru V, Gunduz A, Starr PA, et al. Proceedings of the Sixth Deep Brain Stimulation Think Tank Modulation of Brain Networks and Application of Advanced Neuroimaging, Neurophysiology, and Optogenetics. Front Neurosci 2019;13:1–21. doi:10.3389/fnins.2019.00936. [PubMed: 30740042]

[61]. Starr PA. Totally implantable bidirectional neural prostheses: A flexible platform for innovation in neuromodulation. Front Neurosci 2018;12:1–5. doi:10.3389/fnins.2018.00619. [PubMed: 29403346]

Highlights:

- Single-pulse electrical stimulation was delivered via intracranial electrodes to a range of brain regions in patients undergoing long-term monitoring
- Stimulation intensities of 5.5 mA and higher produced a consistent corticocortical evoked potential (CCEP) and evoked gamma-band (70-150 Hz) power response up to 100 ms post-stimulation
- Hippocampus showed the largest response across areas and patients
- The CCEP amplitude was 9.9% larger and the evoked gamma-band response was 120.0% larger in the clinical seizure onset zone compared with areas outside this zone

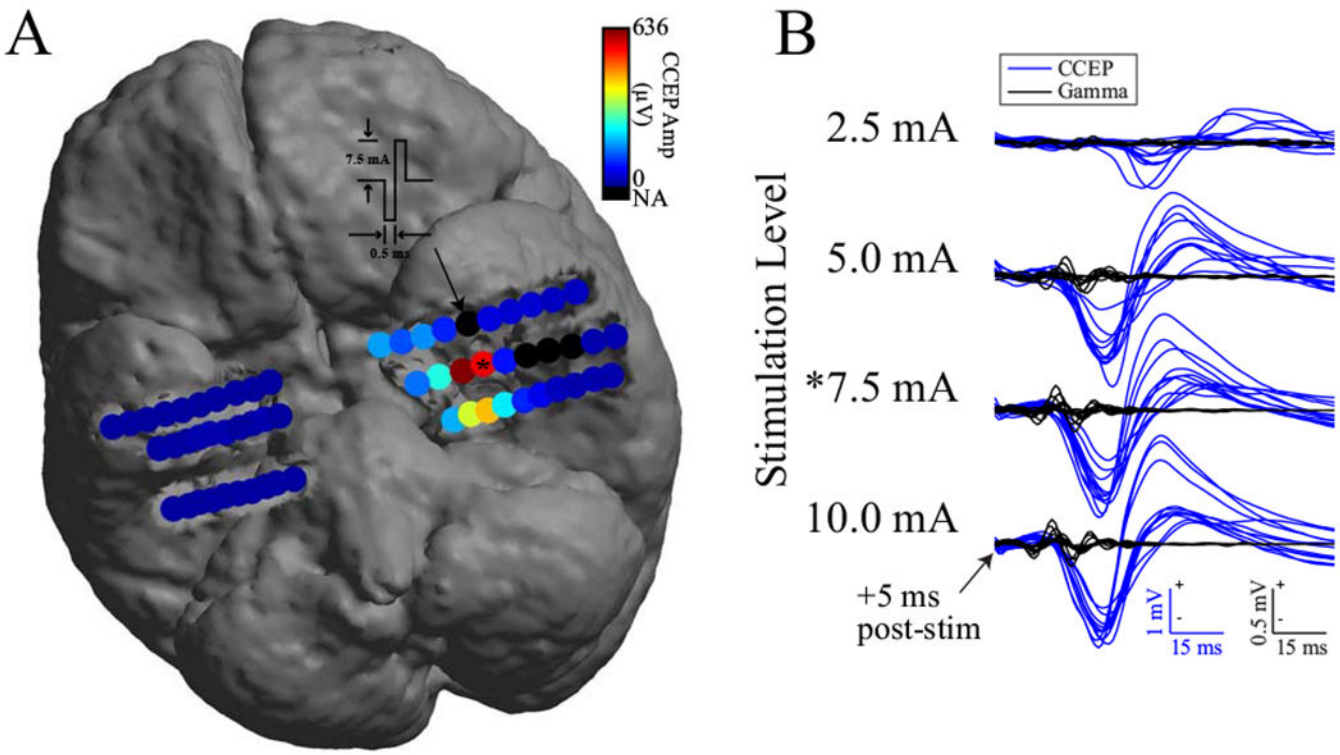

Figure 1.

CCEP response pattern to SPES and single-trial CCEPs and gamma responses across levels. (A) CCEP responses to SPES at 7.5 mA on electrode #5 (denoted by arrow) in left amygdala of patient 3 showing spread to anterior and posterior hippocampal leads. Color indicates mean absolute value of trial average CCEPs from 5 to 100 ms post-stimulation. Black electrodes contained artifact or were disabled. Responses remained ipsilateral to the location of stimulation in this example. (B) Single-trial CCEPs (blue) and gamma responses (black) recorded at 4 stimulation levels on electrode #4 in left hippocampus after SPES on electrode #5 in left amygdala. Asterisk indicates same CCEP data (electrode and level) between A and B. Polarity of voltage or power is marked on figure scale, + is up.

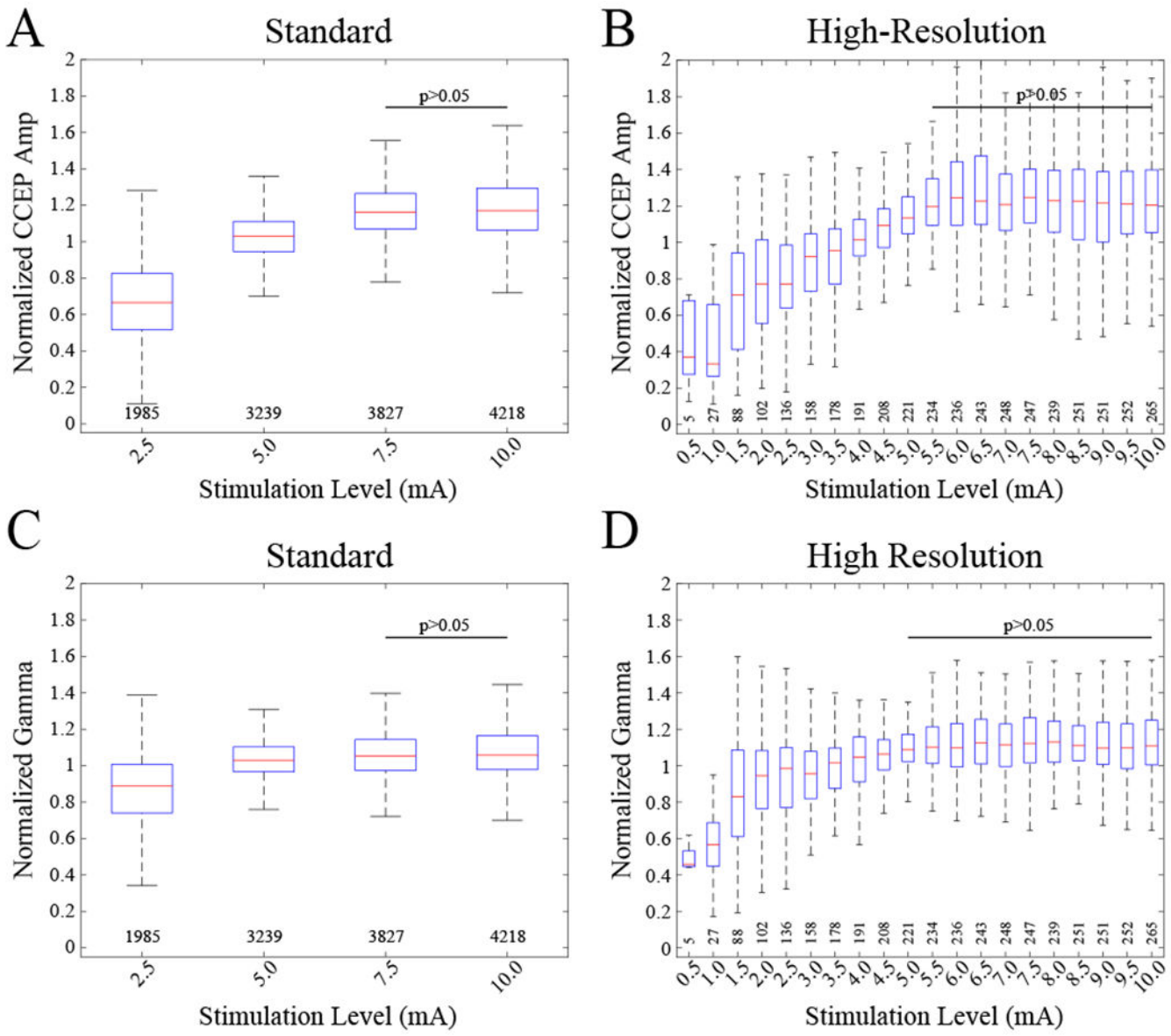

Figure 2.

Normalized CCEP amplitude and gamma power (70-150 Hz) as a function of stimulation level. Boxplots indicate normalized medians, interquartile ranges, and extremes at each level. Normalization was performed by dividing each value by the mean across levels for each unique stimulation-response electrode pair. (A) Normalized CCEP amplitudes across 4 stimulation levels for 7 patients. Raw amplitudes had medians (ranges) of 62 (4-2138), 111 (7-2784), 128 (16-3545), 128 (15-3194) μV for each of the levels, respectively. CCEPs are from 387 stimulated electrodes in amygdala and hippocampus as well as neocortex and white-matter regions of the brain. The number of CCEPs at each level is indicated below each boxplot. Omnibus KW test shows main effect of stimulation amplitude (χ^2=4.97*10^3, df=3, p=0). No difference was found between CCEPs at 7.5 and 10 mA. All other pairwise combinations were significantly different (pairwise rank-sum tests, p<0.05). (B) Omnibus KW test confirms main effect of stimulation amplitude (χ^2=999, df=19, p=7.36*10^{-200}).

CCEP amplitudes across 20 stimulation levels for 6 patients. CCEPs are from 22 stimulated electrodes in amygdala and hippocampus as well as frontal and white-matter regions of the brain. No difference was found for all pairwise combinations of CCEPs at ≥5.5 mA. A trend of decreasing CCEP amplitude for lower values and a plateau-effect for higher values begins at ~5.0 mA. (C) Normalized gamma power across levels for the standard dataset. Omnibus KW test confirms main effect of stimulation amplitude (χ^2=1.37*10^3, df=3, p=3.27*10^{-297}). No difference was found between 7.5 and 10.0 mA for the "standard" and all pairwise combinations of ≥5.0 mA for the "high-resolution" datasets. (D) Normalized gamma power across levels for the "high-resolution" dataset. Omnibus KW test confirms main effect of stimulation amplitude (χ^2=377, df=19, p=2.39*10^{-68}). A plateau-effect begins at ~5.5 mA similar to CCEP amplitude.

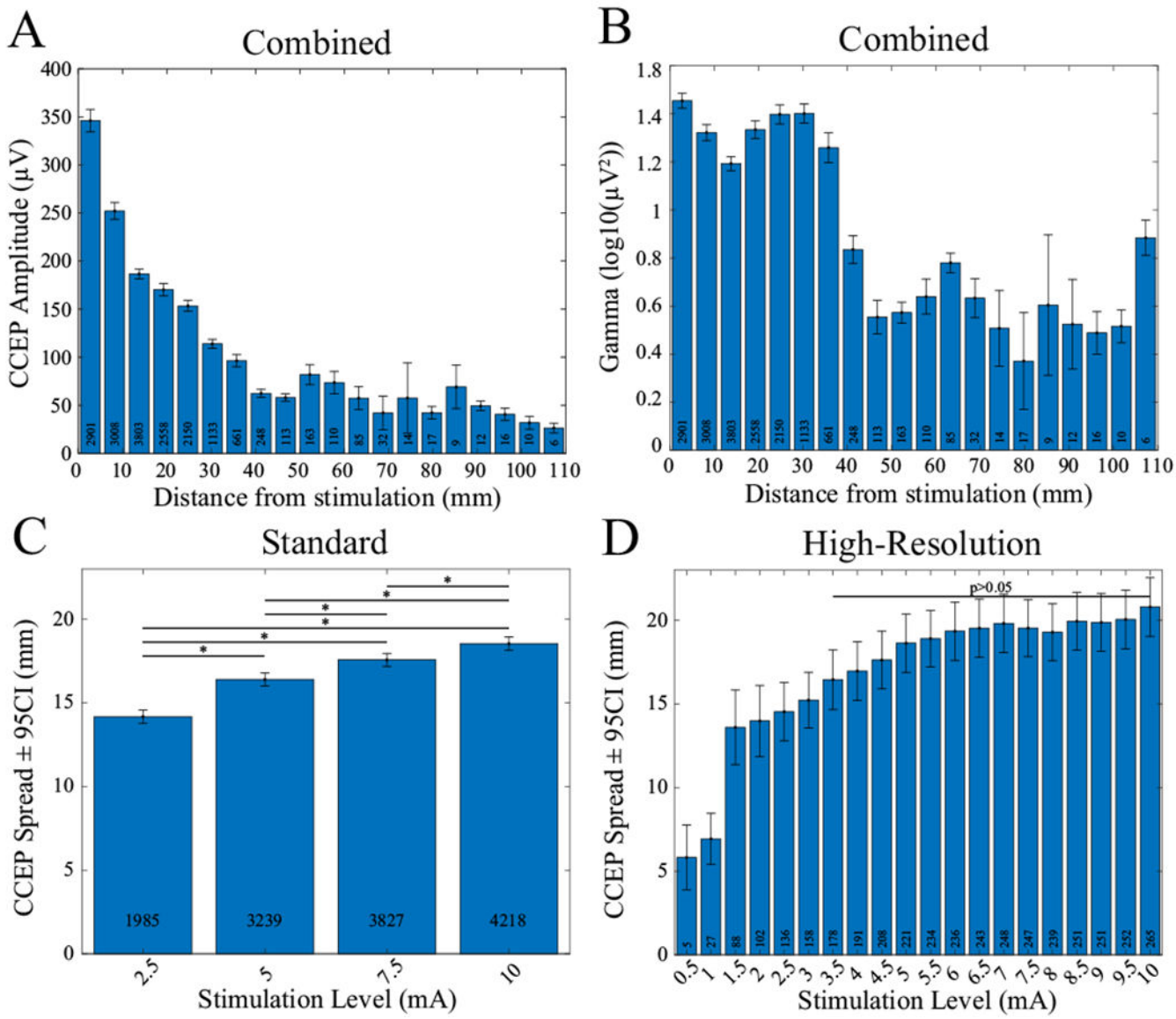

Figure 3.

CCEP amplitude and gamma power as a function of distance. (A) CCEP amplitude versus distance from stimulation combined across all patients and all stimulation levels. A steady decrease in amplitude occurs until ~50 mm. (B) Gamma-band power versus distance across all patients and all stimulation levels. An abrupt drop in power occurs at ~35 mm. (C, D) Spatial spread of CCEPs as a function of stimulation level. Error bars indicate 95% confidence. White boxes indicate total count per bin. C) Mean distance from stimulated electrodes to detected CCEPs across 4 levels and 7 patients. CCEPs are from 387 stimulated electrodes. Distance increases with each level ($p<0.05$). Significant pairwise comparisons are indicated with an asterisk. Mean distances (ranges) for each level are 14.2 (2.4-95.3), 16.4 (2.4-108.1), 17.6 (2.4108.1), 18.5 (2.4-108.1) mm, respectively. (D) Mean distance from stimulated electrodes to detected CCEPs across 20 levels and 6 patients. CCEPs are from 22 stimulated electrodes. No difference was found for all pairwise combinations of

levels ≥3.5 mA. A transition to a plateau occurs at ~5.5 mA similar to CCEP amplitude versus level in Figure 2. A discontinuity occurs between 1 and 1.5 mA. This is because CCEPs at levels <1.5 mA primarily occurred on adjacent electrodes with spacings of ≤5 mm. The range of distances across all levels was 3.5-67.2 mm.

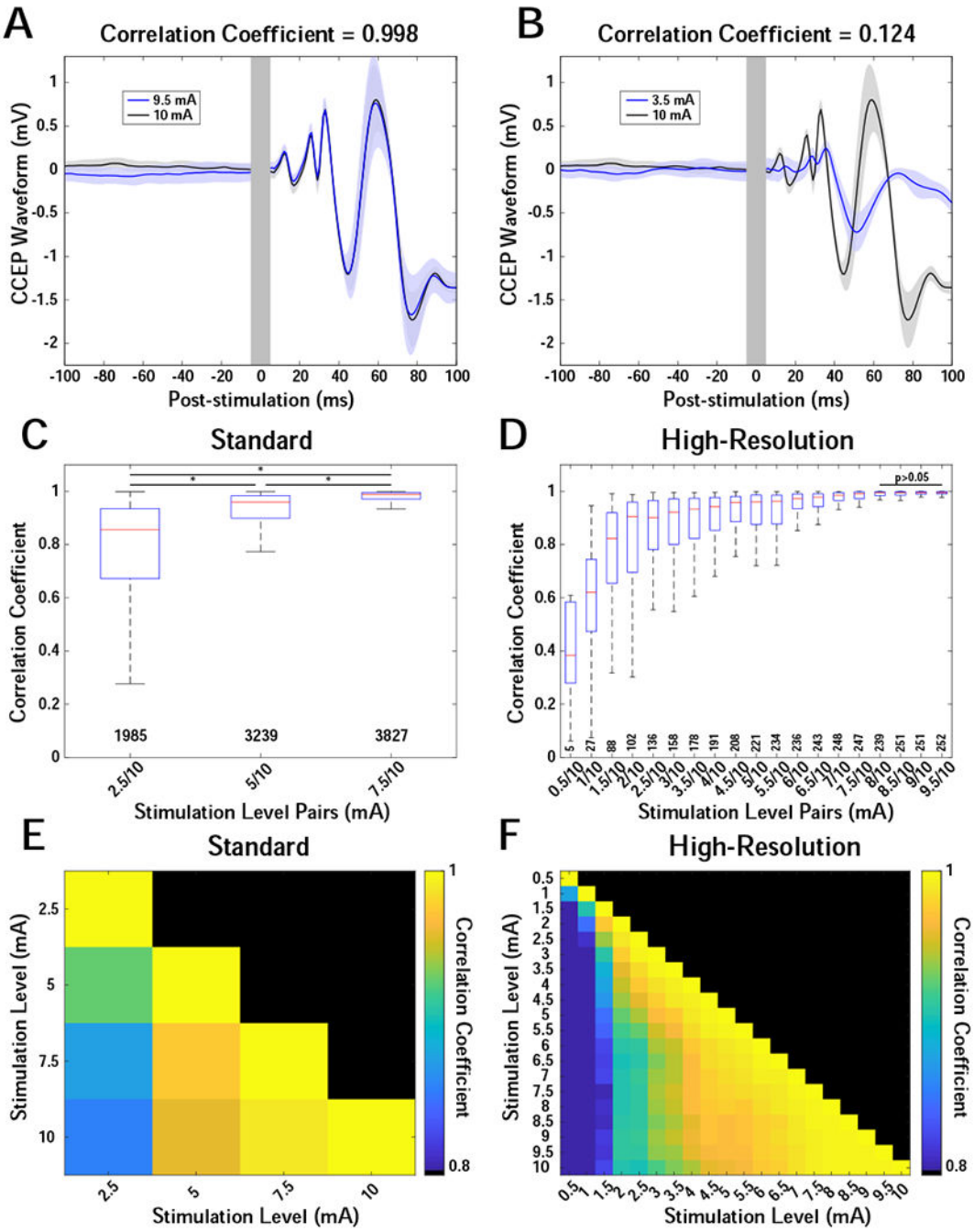

Figure 4.

CCEP waveform shape comparisons across levels. Trial-averaged CCEP waveforms were compared across levels for individual stimulation-response pairs using the Pearson correlation coefficient. (A, B) Example waveforms demonstrating high and low correlations for 9.5 vs 10 mA (A) and 3.5 vs 10 mA (B), respectively. Stimulation was in the amygdala, and the CCEPs were recorded on an electrode in the hippocampus. Solid traces are the trial-average waveforms, and shaded areas indicate 95% confidence. Gray vertical bars indicate artifact region from −5 to 5 ms relative to stimulation. (C) Correlations of 3 levels (2.5, 5,

7.5 mA) compared with 10 mA for 7 patients. Boxplots show medians, interquartile ranges, and outliers for each comparison. Pairwise comparisons of all distributions showed significant differences (pairwise rank-sum test, $p<0.05$) and are indicated with an asterisk. (D) Correlations of 19 levels (0.5 by 0.5 to 9.5 mA) compared with 10.0 mA for 6 patients. No pairwise differences were found for the last 4 distributions (≥8 mA). Interquartile range demonstrates a transition to lower values at a level ≥~5.5 mA. (E,F) Heatmaps showing the median correlation for all pairwise combinations of levels for both the “standard” (E) and “high-resolution” (F) datasets. Color indicates median correlation coefficient scaled from 0.8 to 1. X- and Y-axes indicate level combination.

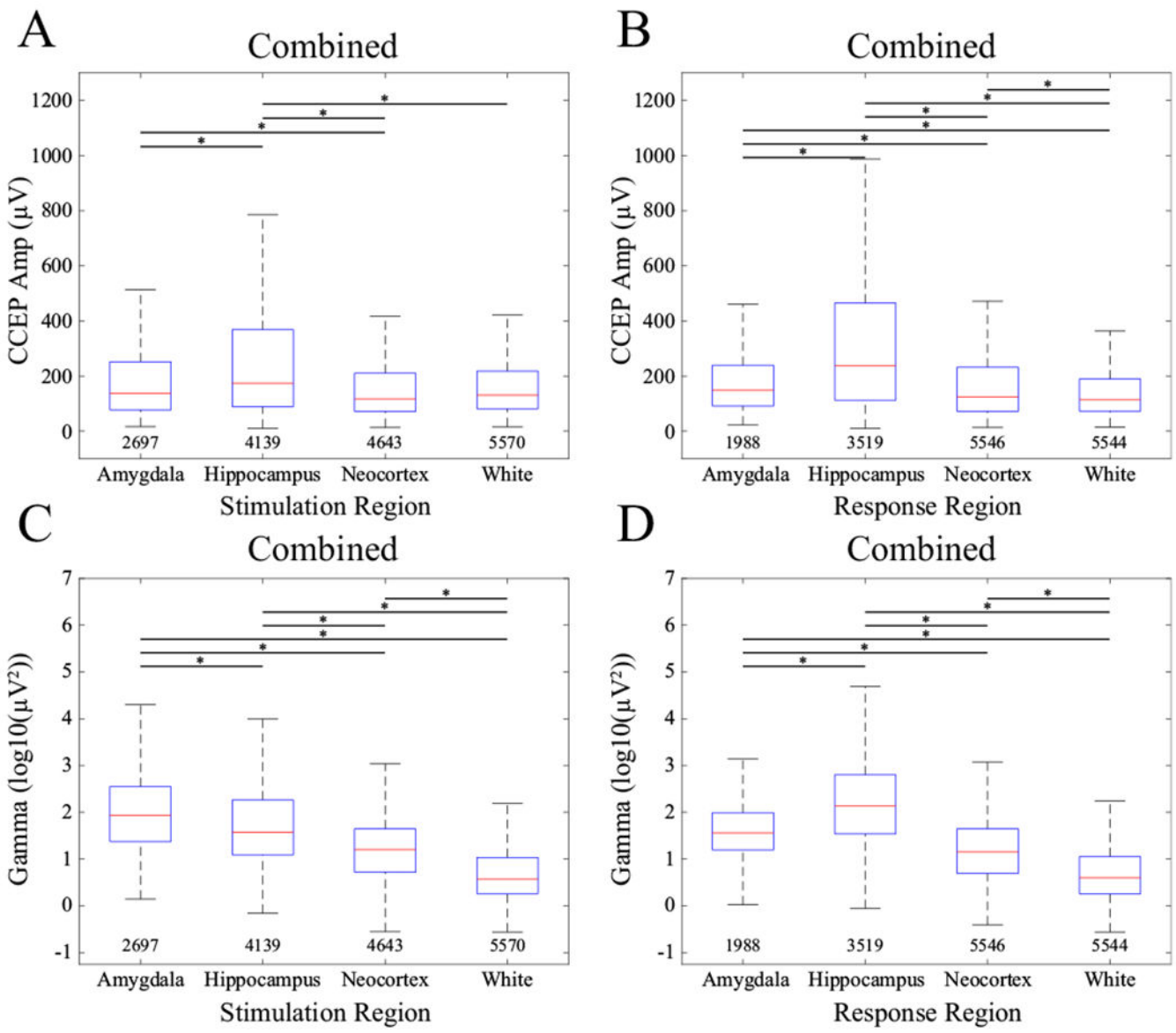

Figure 5.

CCEP amplitude (A, B) and gamma power (C, D) comparisons by region of stimulation (A, C) and region of response (B, D). Asterisks show pairwise significance (pairwise rank-sum tests, $p<0.05$, Tukey-Kramer corrected). Numbers below each boxplot indicate count. Data were combined across all stimulation levels and all patients.

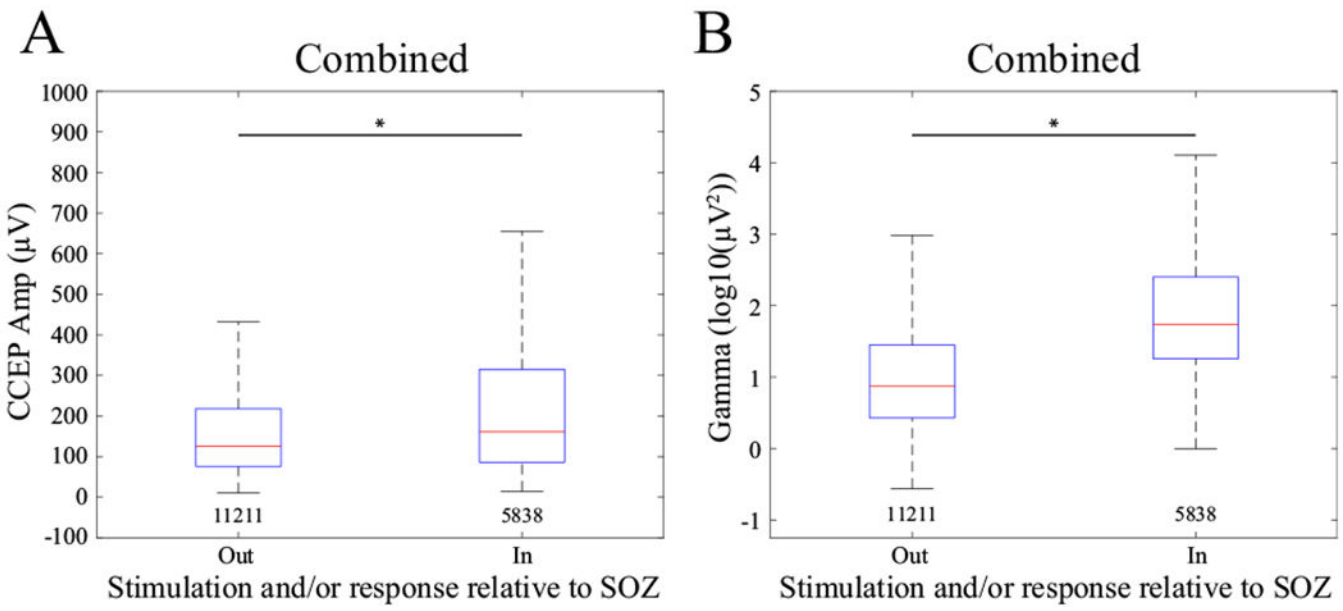

Figure 6.

(A) CCEP amplitude and (B) gamma power response relative to whether the stimulation or response electrode or both were in the SOZ. Asterisks show significant difference between groups as defined by the model. Numbers below each boxplot indicate the count. Data were combined across all stimulation levels and all patients.

Table 1.

Patient demographics

Patient ID	Age (y)	Sex	Seizure focus	Number of stimulation electrodes	Number of response electrodes	Intervention
1	42	F	Bilateral temporal	58	60	RNS
2	41	M	R temporal	51	57	R ATL
3	38	M	Bilateral temporal	57	57	RNS
4	31	F	L temporal	60	60	RNS
5	50	M	Not applicable	56	59	VNS
6	39	M	Bilateral temporal	49	49	None
7	20	M	Bilateral hippocampi *	56	79	RNS
8	21	M	Not applicable	4	33	VNS
9	30	F	L hippocampus	4	38	LITT
10	38	F	Not applicable	2	41	ANT stimulation
11	31	F	R frontal	2	15	R frontal resection

F: female; M: male; R: right; L: left; RNS: responsive neurostimulation; ATL: Anterior temporal lobectomy; VNS: vagal nerve stimulation; LITT: laser interstitial thermal therapy; ANT: anterior nucleus of the thalamus

* Note for patient 7, only the left hippocampus showed ictal activity in particular contacts, thus only left contacts are labelled as part of the seizure onset zone (SOZ) in the data. The right hippocampus was also suspected to be part of the SOZ based on interictal data, however, to be conservative, no right-sided contacts are marked as the SOZ in the dataset.

Table 2.

Results of CCEP model

Name predictor	Estimate	SE	t	DF	p Value	Lower	Upper
(Intercept)	5.1574	0.1644	31.3798	156925	0.0000 *	4.8353	5.4795
Stim level (μA)	$2.8*10^{-5}$	$6.8e^{-6}$	4.0982	156925	0.0000 *	$1.5*10^{-5}$	$4.1*10^{-5}$
Distance (mm)	−0.0292	0.0001	−211.8870	156925	0.0000 *	−0.0295	−0.0290
SOZ true	0.0939	0.0045	21.0684	156925	0.0000 *	0.0852	0.1027
Region response type (Amygdala as reference)							
Hippocampus	0.5752	0.0065	88.5116	156925	0.0000 *	0.5624	0.5879
Neocortex	0.0996	0.0068	14.6349	156925	0.0000 *	0.0862	0.1129
White matter	−0.0872	0.0061	−14.3814	156925	0.0000 *	−0.0991	−0.0753
Region stimulation type (Amygdala as reference)							
Hippocampus	0.2266	0.0055	41.1040	156925	0.0000 *	0.2158	0.2374
Neocortex	0.0099	0.0069	1.4319	156925	0.1522	−0.0036	0.0234
White matter	−0.0018	0.0053	−0.3284	156925	0.7426	−0.0122	0.0087

CCEP amplitude as a function of stimulation intensity, distance between stimulation and response electrodes, region of stimulation, region of response, and SOZ SE, standard error; DF, degrees of freedom; Stim, stimulation; SOZ, seizure onset zone

* Significant at $p<0.0001$.

Table 3.

Results of gamma power model

Name predictor	Estimate	SE	t	DF	p Value	Lower	Upper
(Intercept)	4.5361	0.3757	12.0733	156925	0.0000 *	3.7997	5.2725
Stim level (μA)	$2.84*10^{-5}$	$7.5*10^{-6}$	3.7786	156925	0.0002	$1.4*10^{-5}$	$4.3*10^{-5}$
Distance (mm)	−0.0251	0.0003	−78.8031	156925	0.0000 *	−0.0257	−0.0245
SOZ true	0.7885	0.0103	76.7152	156925	0.0000 *	0.7683	0.8086
Region response type (amygda a as reference)							
Hippocampus	1.5181	0.0150	101.3300	156925	0.0000 *	1.4888	1.5475
Neocortex	0.0276	0.0157	1.7572	156925	0.0789	−0.0032	0.0583
White matter	−0.8077	0.0140	−57.7752	156925	0.0000 *	−0.8351	−0.7803
Region stimulation type (amygdala as reference)							
Hippocampus	−0.9910	0.0127	−77.9814	156925	0.0000 *	−1.0159	−0.9661
Neocortex	−1.6492	0.0159	−103.4836	156925	0.0000*	−1.6804	−1.6180
White matter	−2.0578	0.0123	−167.4105	156925	0.0000 *	−2.0819	−2.0337

Gamma power amplitude as a of stimulation intensity, distance between stimulation and response electrodes, region of stimulation, region of response, and SOZ SE, standard error; DF, degrees of freedom; Stim, stimulation; SOZ, seizure onset zone

*Significant at $p<0.0001$.